Research Article

SCI

Received: 18 December 2015 Revised: 26 February 2016 Accepted article published: 4 March 2016 Published online in Wiley Online Library:

(wileyonlinelibrary.com) DOI 10.1002/pi.5101

Integrated three-dimensional fiber/hydrogel biphasic scaffolds for periodontal bone tissue engineering

Dario Puppi,[a] Chiara Migone,[a] Lucia Grassi,[a] Alessandro Pirosa,[a] Giuseppantonio Maisetta,[b] Giovanna Batoni[b] and Federica Chiellini[a]*

Abstract

Combining a tissue engineering scaffold made of a load-bearing polymer with a hydrogel represents a powerful approach to enhancing the functionalities of the resulting biphasic construct, such as its mechanical properties or ability to support cellular colonization. This research activity was aimed at the development of biphasic scaffolds through the combination of an additively manufactured poly(ε-caprolactone) (PCL) fiber construct and a chitosan/poly(γ-glutamic acid) polyelectrolyte complex hydrogel. By investigating a set of layered structures made of PCL or PCL/hydroxyapatite composite, biphasic scaffold prototypes with good integration of the two phases at the macroscale and microscale were developed. The biphasic constructs were able to absorb cell culture medium up to 10-fold of their weight, and the combination of the two phases had a significant influence on compressive mechanical properties compared with hydrogel or PCL scaffold alone. In addition, due to the presence of chitosan in the hydrogel phase, biphasic scaffolds exerted a broad-spectrum antibacterial activity. The developed biphasic systems appear well suited for application in periodontal bone regenerative approaches in which a biodegradable porous structure providing mechanical stability and a hydrogel phase functioning as absorbing depot of endogenous proteins are simultaneously required.

Keywords: tissue engineering; biphasic scaffold; poly(ε-caprolactone); chitosan; poly(γ-glutamic acid)

INTRODUCTION

Periodontal diseases are usually caused by pathogenic microbes forming a bio-film which is difficult to eradicate leading to inflammatory disorders such as gingivitis and periodontitis.[1,2] In addition, genetic and environmental factors as well as different diseases (e.g. dermatological and haematological) can contribute to periodontal disorders. In the case of periodontitis, the inflammation expands deep into the tooth-surrounding tissues and can result in loss of teeth and degeneration of supporting connective tissue and alveolar bone.[3] While traditional periodontal treatments aim to remove the causes of the occurring infection, the ultimate goal of tissue engineering is regenerating the tissue defect.[4] Given the complex and hierarchically structured nature of periodontal tissue, tissue engineering faces the repair of a variety of tissues including alveolar bone, periodontal ligament, cementum and gingival tissue.[5] A growing body of research has been focused on the development of periodontal polymeric scaffolds, such as injectable hydrogels or three-dimensional (3D) porous constructs.[6] As examples, calcium-phosphate-coated melt-electrospun poly(ε-caprolactone) (PCL) meshes were investigated as scaffolds for periodontal bone regeneration in combination with decellularized[7] or intact[8] periodontal ligament cell sheets to achieve periodontal attachment formation and cementum regeneration. Strategic biomimicry could be imparted through the use of multiphasic scaffolds designed for functional integration of the different periodontal soft and hard tissue components with one another or with the host environment.[9] With this aim, various strategic scaffold multiphasic architectures have been developed: bone scaffolds combined with an occlusive membrane,[10,11] layered biphasic scaffolds for bone and ligament compartments[12–16] and layered triphasic scaffolds for cementum, periodontal ligament and bone compartment.[17]

Regenerative approaches toward *in situ* periodontal tissue regeneration are frequently based on endogenous resources such as cells and growth factors.[4] The most exploited strategy involves a scaffolding material (e.g. fibrin, collagen and Emdogain® gel) in combination with autogenic growth factors, used either to recruit host stem cells or to inject encapsulated autogenic cells (e.g. gingival stem cells[18] or fibroblasts[19]). A reliable alternative that has found clinical translation for periodontium regeneration treatments involves the functionalization of a scaffold with platelet-rich plasma (PRP), an autologous platelet concentrate prepared from patient's own blood as a source of key endogenous growth factors and proteins. As recently reviewed,[20,21] a number of clinical trials have shown that PRP could be combined with different materials

* *Correspondence to: F Chiellini, Department of Chemistry and Industrial Chemistry, University of Pisa, Via G. Moruzzi 13, 56124 Pisa, Italy. E-mail: federica.chiellini@unipi.it*

a *BIOLab Research Group, Department of Chemistry and Industrial Chemistry, University of Pisa, UdR INSTM Pisa, Pisa, Italy*

b *Department of Translational Research and New Technologies in Medicine and Surgery, University of Pisa, Pisa, Italy*

such as bovine xenograft,[22] bioactive glass,[23] hydroxyapatite[24] and β-tricalcium phosphate[25] to achieve enhanced healing of human intrabony defects. Platelet-rich fibrin is a second generation platelet concentrate consisting of a strong natural fibrin matrix prepared from the patient's own blood by centrifugation without using any anticoagulant or other artificial biochemical modifications. This approach has found clinical application in periodontal tissue regeneration thanks to the possibility of obtaining directly from the blood a fibrin gel which concentrates almost all the platelets and growth factors of the blood specimen.[26]

PCL is a biodegradable polyester widely investigated for biomedical applications because of its good biocompatibility, inexpensive production routes, tunable biodegradation kinetics and mechanical properties, and good blend compatibility.[27] In addition, thanks to its good rheological and viscoelastic properties, PCL has been successfully processed into a wide range of porous scaffolds structured at the microscale and nanoscale.[28] For instance, PCL layered microfibrous structures[29] and nanofibrous assemblies[30] were recently investigated as bone tissue engineering scaffolds. However, the slow biodegradation (years for complete *in vivo* absorption[31]) of PCL could limit its application as a biodegradable implant for periodontal applications. In fact, as pointed out by Rasperini *et al.*,[16] a more rapidly resorbing scaffold would be better suited for the treatment of a periodontal osseous defect to avoid wound dehiscence and subsequent microbial contamination in the perimucosal environment around teeth. In addition, being hydrophobic in nature, polyesters like PCL cannot be directly functionalized with platelet concentrates to develop bioactive scaffolds for endogenous regenerative treatments. The strategy followed in this study to overcome such drawbacks was to combine a low molecular weight PCL processed into a highly porous scaffold with a hydrogel phase with a faster degradation rate and swelling properties.

Hydrogels have attracted great interest as scaffolding material owing to their ability to absorb aqueous medium up to thousands of times their dry weight, to encapsulate cells and bioactive molecules as well as to allow efficient mass transfer.[32] In addition, hydrogels based on polymers from natural resources possess inherent biocompatibility, biodegradability and biologically recognizable moieties that could support cellular activities. Chitosan/poly(γ-glutamic acid) (CS/γ-PGA) hydrogels represent a successful example of 3D swollen structures obtained through ionic complexation of two naturally derived polymers.[33,34] However, typical shortcomings of hydrogels limiting their application for biomedical purposes are their mechanical weakness and lack of mechanical integrity, poor control over pore size and difficulty of directly shaping them in predesigned geometries by additive manufacturing (AM).[35]

This study aims to contribute to the growing area of periodontal bone tissue engineering research by exploring the development of biphasic scaffolds composed of a layered PCL porous construct obtained by computer-aided wet-spinning (CAWS) and a CS/γ-PGA polyelectrolyte complex (PEC) hydrogel. As recently reported,[29] with the CAWS technique layer-by-layer PCL and PCL/hydroxyapatite (HA) nanocomposite scaffolds were fabricated with customized external shape and internal fully interconnected porous architecture that well supported bone regeneration processes *in vitro*. Cell culture experiments employing the MC3T3-E1 preosteoblast cell line showed good cell adhesion, proliferation, alkaline phosphatase activity and bone mineralization on the developed PCL-based scaffolds.[29] CS/γ-PGA PEC hydrogels are characterized by a high swelling degree and stability in aqueous solutions as well as the ability to support *in vitro* BALB/3 T3 mouse embryo fibroblast adhesion and proliferation.[33,34] Therefore, the specific objective of this study was to couple the mechanical strength, slow degradation and controlled porous microstructure of PCL-based scaffolds to the swelling properties of a CS/γ-PGA hydrogel exploitable for protein absorption in regenerative medicine approaches. To this end, a novel experimental procedure for combining the two phases by immersion of a PCL-based scaffold into a CS/γ-PGA mixture was explored. PCL and PCL/HA scaffolds with different pore sizes and CS/γ-PGA mixtures with different compositions were investigated to develop a set of biphasic polymeric constructs. Biphasic scaffold prototypes were characterized for their morphology by SEM, thermal properties by TGA and DSC, swelling properties in cell culture medium 1× at 37 °C, and compressive mechanical properties with a uniaxial testing machine. In addition, the antibacterial activity of the biphasic constructs was tested against *Staphylococcus epidermidis* and *Escherichia coli*, selected as representative species of Gram-positive and Gram-negative bacteria, respectively.

EXPERIMENTAL

Materials

PCL (CAPA 6500, $M_w = 50\,000$ g mol^{-1}) was supplied by Perstorp Caprolactones Ltd (Warrington, UK). CS (medium molecular weight, $M_w = 108$ kDa, deacetylation degree *ca* 92%) and HA nanoparticles (size <200 nm) were bought from Sigma Aldrich (Milan, Italy). γ-PGA (100 kDa) was obtained from Natto Bioscience (Osaka, Japan).

Preparation of PCL and PCL/HA scaffolds

PCL pellets were dissolved in acetone at 35 °C for 2 h under gentle stirring to obtain a homogeneous solution at the desired concentration (20% w/v). For the production of PCL/HA composite scaffolds, HA nanoparticles (1:4 HA/PCL weight ratio) were added to the polymeric solution and left under vigorous stirring at 35 °C for 1 h until a homogeneous dispersion of the nanoparticles was achieved. Scaffold manufacturing was performed by means of a computer-controlled rapid prototyping machine (MDX-40A, Roland DG Mid Europe Srl, Ascoli Piceno, Italy), modified in-house to allow the production of 3D scaffolds composed of wet-spun polymeric fibers.[36] The prepared solution was placed in a plastic syringe fitted with a stainless steel blunt needle, inner diameter 0.41 mm (gauge 22). A syringe pump (NE-1000, New Era Pump Systems, Wantagh, NY, USA) was used to control the extrusion flow rate of the polymer solution into the coagulation bath. A beaker containing ethanol was fixed to the fabrication platform and used as a coagulation bath. The 3D geometrical scaffold parameters, including the distance between the fiber axis (d_{xy}), layer thickness, scaffold external geometry and sizes, were designed using an algorithm developed in Matlab software (Mathworks Inc. Natik, MA, USA). The combination of the X–Z axis needle motion and the Y axis platform motion allowed the fabrication of scaffolds layer-by-layer. The manufactured scaffolds were removed from the coagulation bath, kept under a fume hood overnight and then in a vacuum chamber for 48 h.

Preparation of biphasic scaffolds

CS/γ-PGA mixtures (80:20 weight ratio) were prepared by dissolving γ-PGA in dH_2O under stirring for 1 h at room temperature.

The desired amount of CS was then added to the γ-PGA solution, and the suspension was left under vigorous stirring for 2 h. Acetic acid (1% v/v) was finally added and the mixture obtained was left overnight with stirring. The total concentration of the polymeric phase in the mixture was either 5% or 2.5% w/v. For the preparation of biphasic scaffolds, PCL and PCL/HA wet-spun samples were placed in a 12-well tissue culture plate, covered with CS/γ-PGA solution (4 mL for each sample) and left 5 h at room temperature. The PCL-based scaffolds were periodically turned upside down to allow a good infiltration of the solution into the scaffold pores. The samples were then frozen at −20 °C for 24 h, lyophilized for 72 h (−50 °C, 0.04 Torr) and stored in a desiccator.

Morphological characterization

The morphology of the developed scaffolds was analyzed using SEM with a JEOL LSM 5600LV microscope (Tokyo, Japan) under backscattered electron imaging. The fiber diameter and pore size were measured by means of ImageJ 1.43u software (National Institutes of Health, Bethesda, MD, USA) on SEM micrographs with 35× magnification. Data were calculated over 20 measurements per scaffold.

Determination of swelling degree

A swelling study of the prepared samples was carried out in Dulbecco's modified Eagle's medium (DMEM) (Sigma Aldrich). At different time intervals, the samples were weighed after wiping the swelling medium from the surface with filter paper. Experiments were performed in triplicate and the percentage swelling degree (SD) was calculated as

$$SD = \left[\left(W_s - W_d\right)/W_d\right] \times 100$$

where W_d is the weight of the dry sample and W_s is the weight of the swollen sample.

Thermal characterization

TGA was performed using a TGA Q500 instrument (TA Instruments, Milan, Italy) under a constant nitrogen flow of 60 mL min^{-1}, in the temperature range 25–600 °C, and at a constant heating rate of 10 °C min^{-1}. The onset temperature (T_{onset}), given by the intersection of the tangent to the baseline with the tangent to the inflection point of the TGA curve, was considered as the starting degradation temperature. DSC analysis was performed in the range −100 to 200 °C at a heating rate of 10 °C min^{-1}, a cooling rate of 10 °C min^{-1} and under a nitrogen flow rate of 80 mL min^{-1}, using a Mettler DSC-822E instrument (Mettler Toledo, Milan, Italy). The glass transition temperature (T_g) was evaluated by analyzing the inflection point, while the melting temperature (T_m) and percentage crystallinity (C%) were evaluated by analyzing the endothermic peaks in the DSC heating scans. Three samples for each kind of scaffold were tested in both thermal analyses.

Mechanical characterization

The compressive mechanical properties of the scaffolds were analyzed using a uniaxial testing system (Instron 5564, Norwood, MA, USA) with a 2 kN load cell. The test was conducted in air at room temperature after 8 h of submersion in PBS 1×; PCL and PCL/HA scaffolds with a square base area of 10 × 10 mm^2 and a thickness of about 5 mm (50 layers) and biphasic scaffolds with a cylindrical geometry (diameter about 20 mm and thickness about 7 mm) were tested. Five samples of each kind of scaffold were characterized at a crosshead speed of 1 mm min^{-1} between two parallel steel plates up to a maximum strain of 90%. The stress was defined as the measured force divided by the total area of the apparent cross-section of the scaffold, whilst the strain was evaluated as the ratio between the scaffold height variation and its initial height. The compressive modulus was calculated from the stress–strain curves as the slope of the initial linear region. Representative stress values taken at 50% and 90% of strain were reported in order to quantitatively support the graphical observation that PCL scaffolds were reinforced at high strain by the presence of an infiltrated hydrogel phase.

Antibacterial activity assay

The antibacterial activity of the biphasic scaffolds was evaluated against *S. epidermidis* (ATCC 35984) as a model of Gram-positive bacteria and *E. coli* (ATCC 25922) as a model of Gram-negative bacteria. Bacterial cells were cultured in Mueller–Hinton broth (MHB) (Oxoid, Basingstoke, UK) for 18 h at 37 °C and subsequently diluted in fresh medium and grown until the exponential phase was reached. A volume of 200 μL of each bacterial suspension, containing approximately 2×10^6 colony forming units, was added to 20 mL of MHB in the presence of PCL (or PCL/HA) scaffold, biphasic scaffolds or CS/γ-PGA hydrogel. Bacteria suspended in MHB alone were used as cell growth control. Samples were incubated at 37 °C with shaking for 6 h (for *E. coli*) or 8 h (for *S. epidermidis*), taking into account the growth rate of each bacterial strain. At different times of incubation, the density of the bacterial cultures was determined by measuring the optical density at 600 nm (OD_{600}) using a UV–visible spectrophotometer (GeneQuant Pro, Pharmacia, Uppsala, Sweden).

Statistical analysis

The data are represented as mean ± standard deviation. Statistical differences were analyzed using one-way analysis of variance (ANOVA), and a Tukey test was used for *post hoc* analysis. A P value <0.05 was considered statistically significant.

RESULTS AND DISCUSSION

Biphasic scaffold development

An experimental procedure for the preparation of biphasic constructs composed of an additively manufactured 3D PCL-based porous structure and a hydrogel phase made of a CS/γ-PGA PEC was developed. On the basis of a previous study regarding the development of a CAWS technique for the layered manufacturing of scaffolds made of PCL ($M_w = 80\,000$),[29] the processing conditions for obtaining 3D structures made of a PCL with a lower M_w (50 000 g mol^{-1}) were investigated. The manufacturing process involved the continuous extrusion of a polymeric solution through a needle immersed in an ethanol coagulation bath. 3D scaffold architectures were built up with a layer-by-layer process by depositing the solidifying filament with a 0°–90° lay-down pattern (Fig. 1(a)).The optimized PCL scaffold fabrication parameters were polymer concentration 20% w/v, initial needle tip to collection platform distance 2 mm, deposition velocity 240 mm min^{-1}, solution feed rate 1 mL h^{-1} and inter-layer needle translation 0.1 mm. By applying these parameters, prototypal PCL scaffolds with different pore sizes were developed by changing the inter-fiber needle translation distance (d_{xy}) in the range 0.5 – 2 mm (Fig. 1(b)).

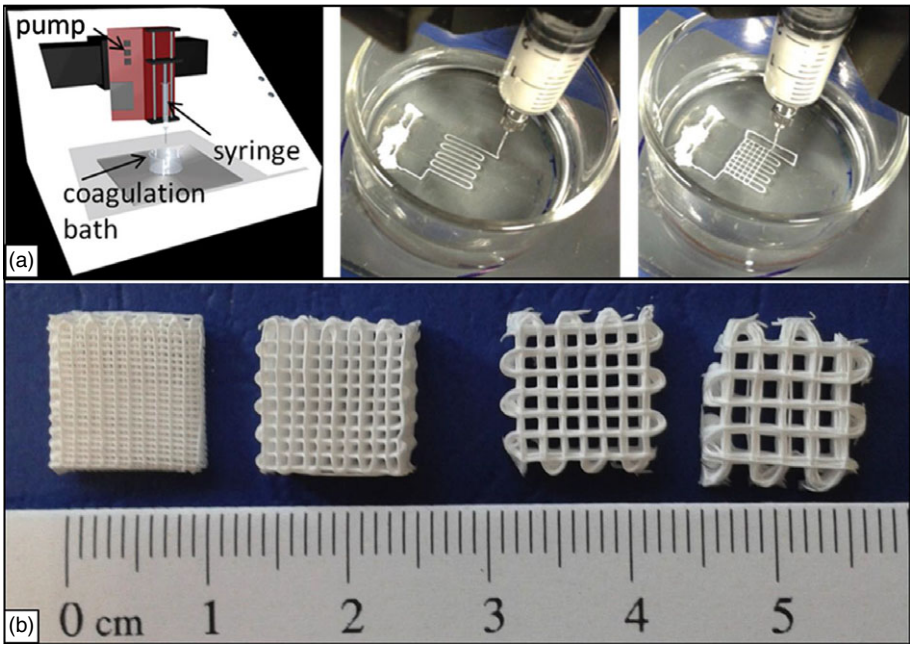

Figure 1. PCL scaffold fabrication by computer-aided wet-spinning (CAWS): (a) schematics of the CAWS apparatus and layer-by-layer production process; (b) PCL scaffolds (10 × 10 mm, 50 layers) with different pore size due to variation in the inter-fiber needle translation (from left to right $d_{xy} = 0.5$, 1, 1.5 and 2 mm).

HA-loaded PCL scaffolds with the same structural characteristics were manufactured by applying the optimized processing parameters to polymeric solutions containing the inorganic particles as suspension (Fig. 2(a)). Biphasic constructs were developed by immersing PCL-based scaffolds in a CS/γ-PGA solution followed by freeze drying. As shown in Fig. 2(b), a too high CS/γ-PGA solution concentration did not allow the required integration to be achieved between the two phases. However, by decreasing the CS/γ-PGA concentration to 2.5% w/v, the hydrogel phase fully penetrated into the PCL porous architecture leading to the formation of an integrated biphasic structure (Fig. 2(c)). By employing this concentration, four biphasic construct prototypes based on either PCL or PCL/HA scaffolds in combination with a CS/γ-PGA hydrogel were developed (Fig. 2(d)). In the dry state the hydrogel portion of the biphasic scaffolds was physically spongy and could be easily handled without breaking. Scaffolds obtained applying $d_{xy} = 0.5$ mm ($PCL_{0.5mm}$ and $PCL/HA_{0.5mm}$) were excluded from the study since the small pore size did not allow good hydrogel penetration even in the case of low solution concentration. In addition, PCL scaffolds with $d_{xy} = 2$ mm (PCL_{2mm} and PCL/HA_{2mm}) were not further investigated because of the flattened fiber morphology at the crossing points leading to the collapse of the 3D structure along the *Z* axis.

The combination of a fibrous polymeric network and a hydrogel phase can represent a powerful tool for the optimization of overall scaffold functionalities, such as mechanical properties, cellular colonization and swelling properties. It can also be seen as a biomimetic approach aimed at the obtainment of a complex composite reproducing the fibrous protein framework supporting the aqueous component in different native tissues.[37] Hydrogels have been combined with a wide array of fibrous structures such as carbon nanotubes,[38,39] polymeric nanofibers[40] and microfibers,[41] polymeric wovens[42,43] and non-wovens,[44] and polymeric layered scaffolds by AM.[37,45–50] For instance, Liao *et al.*[43] developed a potential acellular or cell-based scaffold with

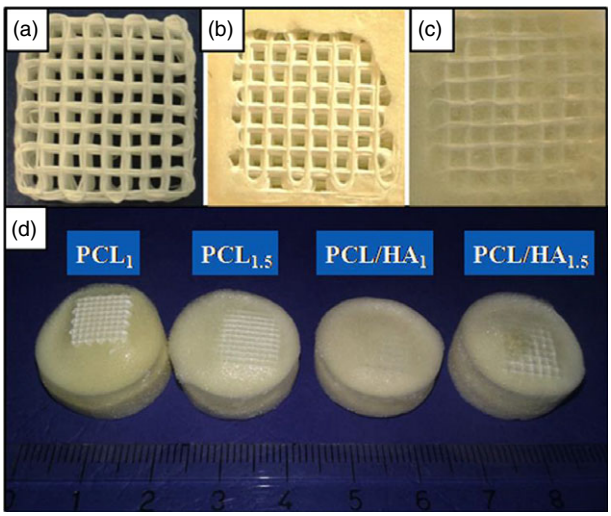

Figure 2. Development of biphasic constructs. Representative photographs of (a) a PCL/HA_1 scaffold, (b) a biphasic construct obtained employing a PCL/HA_1 scaffold and a 5% w/v CS/γ-PGA solution, (c) a biphasic construct obtained employing a PCL/HA_1 scaffold and a 2.5% w/v CS/γ-PGA solution, (d) four biphasic construct prototypes based on PCL or PCL/HA scaffolds in combination with a CS/γ-PGA 2.5% w/v solution (measure unit 1 mm).

tunable mechanical and tribological properties mimicking those of native cartilage, by infiltrating a woven PCL fiber construct with an interpenetrating dual-network 'tough gel' consisting of alginate and polyacrylamide. In another study Yu *et al.*[45] demonstrated that cellular-loading efficiency and cell colonization of layered PCL scaffolds could be enhanced through combination with a stem-cell-seeded collagen hydrogel. The present study makes a noteworthy contribution to this research trend by providing a novel biphasic structure combining layered PCL scaffolds with a PEC hydrogel that could function as a potential depot for

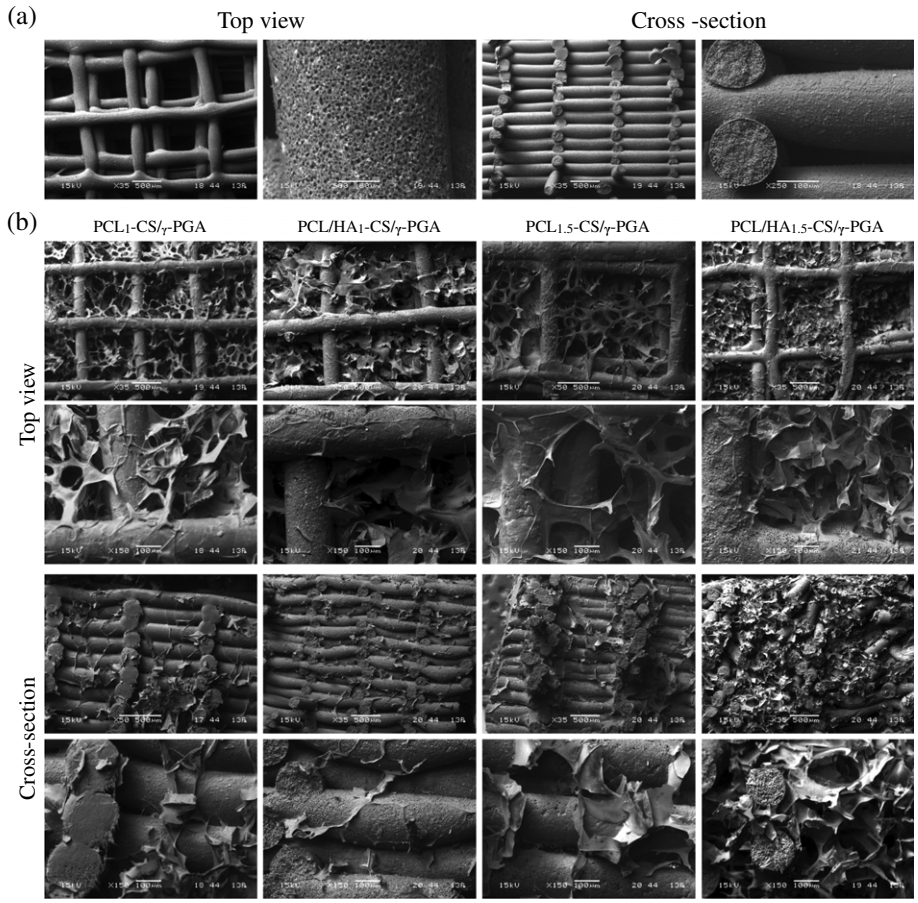

Figure 3. Morphological analysis by SEM. Representative backscattered SEM micrographs taken at different magnifications of the top view and cross-section of (a) PCL_1 scaffolds and (b) biphasic construct prototypes.

endogenous proteins in regenerative approaches. In addition, an integrated hydrogel phase infiltrated into the porous scaffold network enables larger scaffold pore sizes to be employed without potentially compromising the cellular colonization of inter-fiber gaps. Such a system would have faster degradation due to the lower PCL ratio in the biphasic construct. This aspect, together with the employment of a relatively low polymer molecular weight (50 000 g mol^{-1}), can allow the scaffold degradation rate to be increased.

Morphological analysis

SEM image analysis was carried out to assess the integration between the PCL scaffold and the PEC hydrogel on a macroscale and microscale. The morphological investigation highlighted that PCL scaffolds were characterized by a spongy morphology of the deposited fiber constituting the 3D layered structure (Fig. 3(a)).

As widely discussed in previously published papers,[29,36] such microporosity can be ascribed to the phase inversion process governing polymer solidification. In fact, the solvent/non-solvent exchange during polymer solidification leads to the formation of a polymer-rich phase and a polymer-lean phase that will finally result in pore formation in the fiber polymeric matrix. Different from what is commonly obtained by means of melt-extrusion-based AM techniques, the CAWS approach allows hybrid architectures to be developed with both global and local porosity.[51] The resulting fiber microporosity can be tuned in a certain range by acting on different phase inversion parameters (e.g. polymer concentration and deposition velocity). This can allow us to tailor the scaffold biodegradation rate, mass transfer phenomena associated with cell activities and release of loaded drugs, as well as the surface roughness influencing cell adhesion and proliferation.[52]

Dimensional analysis of the scaffold structural parameters revealed a fiber diameter in the range 200–300 μm and an *XY* pore dimension that varied from 200 to 1800 μm by increasing d_{xy} from 0.5 to 2.0 μm (Table 1). The presence of HA nanoparticles in the polymeric matrix did not remarkably influence the two investigated structural parameters. The fiber diameter was not significantly affected by variation in d_{xy}, except in the case of PCL scaffolds obtained with $d_{xy} = 2$ mm characterized by a larger fiber size. This is probably due to fiber flattening at crossing points, strictly related to the shorter layer fabrication time.

SEM analysis corroborated macroscopic observations in highlighting the good integration between the PCL porous scaffold and the hydrogel phase in all the developed biphasic constructs (Fig. 3(b)). The hydrogel phase uniformly infiltrated into the inter-fiber pores and was also clearly visible in the whole scaffold cross-section. As shown in high magnification micrographs, the hydrogel adhered well to the PCL fibers forming a cohesive biphasic interface. In addition, from top view micrographs the porous structure of the hydrogel phase is particularly evident which could be favorable for cell penetration and proliferation.[53]

Table 1. Structural parameters of PCL and PCL/HA scaffolds with different d_{xy}

Scaffold	Inter-fiber needle translation (d_{xy}) (mm)	Fiber diameter (μm)	Pore size[a] (μm)
$PCL_{0.5}$	0.5	238.4 ± 13.4	256.3 ± 36.4
$PCL/HA_{0.5}$	0.5	241.7 ± 21.5	262.3 ± 59.5
PCL_1	1.0	222.1 ± 11.7	812.5 ± 65.4
PCL/HA_1	1.0	240.7 ± 13.4	807.5 ± 41.8
$PCL_{1.5}$	1.5	231.1 ± 14.6	1292.3 ± 45.2
$PCL/HA_{1.5}$	1.5	245.2 ± 16.1	1257.8 ± 61.2
PCL_2	2.0	258.4 ± 16.1[b]	1732.1 ± 52.8
PCL/HA_2	2.0	261.7 ± 21.5[b]	1742.4 ± 53.6

Data expressed as average ± standard deviation ($n = 20$).
[a] Pore sizes of scaffolds with different d_{xy} are significantly different ($P < 0.05$).
[b] Parameters significantly different ($P < 0.05$) in comparison to the other scaffolds with the same composition and different d_{xy}.

Different strategies have been explored to develop biphasic scaffolds made up of a layered load-bearing structure by AM integrated with a hydrogel phase. For instance, bioprinting techniques were applied to manufacture cell-laden constructs by simultaneously[46] or alternatively[47,48] depositing extruded PCL melt and hydrogel. In this case, PCL and hydrogel strands were either combined in each layer or alternatively organized in successive layers. Other papers reported on a procedure similar to that adopted in the current study, involving the soaking of a scaffold in a mold containing a pre-gel solution or the dropping of the hydrogel-forming mixture onto the scaffold.[37,49,50] Although these studies demonstrated the structural reinforcement of the investigated hydrogel by combination with a 3D fibrous structure, they lack a micro-morphological analysis of the construct cross-section as well as the fiber/hydrogel interface. As demonstrated in this study, parameters like hydrogel solution viscosity and fiber scaffold pore size determine the integration of the hydrogel in the porous constructs. In addition, other factors such as electrostatic interactions, polymer hydrophilicity/hydrophobicity and fiber surface roughness influence the adhesion of the hydrogel to the fiber surface. The SEM characterization reported in this research will serve as a basis for future studies on analogous biphasic scaffolds involving a detailed investigation of the actual integration at the macroscale and microscale between the employed hydrogel phase and the fiber network.

Thermal analysis

The thermal properties of the developed scaffolds were investigated to assess the effect of material processing, HA loading and biphasic structure preparation on the PCL macromolecular structure parameters obtained from TGA and DSC analysis. Representative thermograms of the investigated samples are shown in Fig. 4, while the obtained thermal parameters are reported in Table 2.

PCL scaffolds were characterized by a thermal degradation profile overlapping with that of unprocessed PCL (T_{onset} around 385 °C) in agreement with other studies suggesting that CAWS processing does not alter the polymer molecular structure.[36,54] HA-loaded scaffolds had a lower thermal stability ($T_{onset} = 347.26 \pm 11.18$ °C) than plain scaffolds as well as raw polymer, supporting results from previous research on the development of PCL/HA composite scaffolds.[55] The weight residue at 600 °C for PCL/HA_1 scaffolds was 22.20% ± 2.02%. This value can be related to the actual content of the ceramic in the composite and roughly corresponded to the percentage weight of HA added to the polymer solution. CS/γ-PGA PEC hydrogels ($T_{onset} = 293.01 \pm 11.95$ °C) showed faster weight loss in comparison to the two constituting raw polymers (T_{onset} of 306.04 ± 2.08 °C for CS and 359.58 ± 1.38 °C for γ-PGA). This could be mainly related to the evaporation of residual water molecules physically/chemically bound to the polymers as well to a reduced hydrogen bonding density in the CS structure due to the electrostatic interaction with γ-PGA.[56–58] Biphasic constructs (T_{onset} in the range 360–380 °C) exhibited significantly lower thermal stability compared to PCL_1 scaffolds due to the presence of the hydrogel phase.

DSC analysis showed that all the analyzed samples were characterized by an endothermic peak at around 60 °C ascribable to melting of PCL crystalline domains (Fig. 4(b)). The comparative analysis of data from the first scan (Table 2) showed that wet-spun scaffolds had significantly higher T_m and crystallinity than raw polymer. This result is consistent with those of recent studies showing that in the wet-spinning process the non-solvent-induced coagulation generally leads to high levels of polymer crystallinity.[36,54] No statistically significant differences were observed when comparing data sets from the second heating scan of raw PCL, PCL_1 scaffolds and PCL/HA_1 scaffolds, in agreement with what was found during TGA analysis, suggesting that the employed materials processing technique did not cause remarkable chemical-physical changes in polymer structure. T_m and crystallinity obtained from the endothermic peaks of biphasic scaffold traces are statistically comparable to those of PCL_1 scaffolds. It can therefore

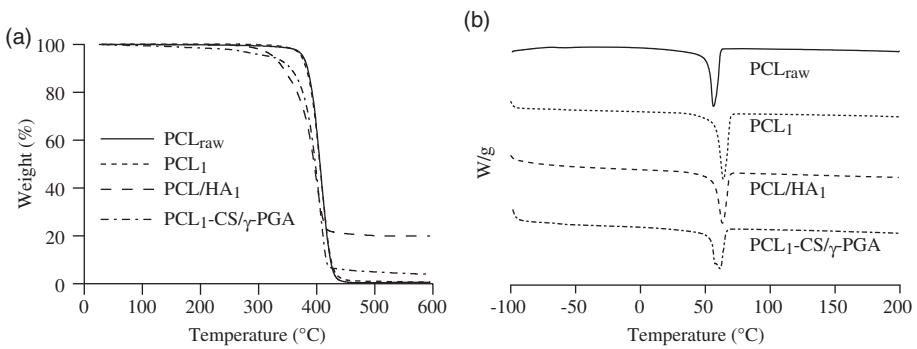

Figure 4. Thermal properties assessment. Representative TGA (a) and first heating DSC (b) thermograms of raw PCL, PCL_1, PCL/HA_1 and PCL-CS/γ-PGA scaffolds.

Table 2. Thermal parameters obtained from TGA and DSC analysis

Sample	T_{onset} (°C)	T_g (°C)		T_m (°C)		Crystallinity (%)	
		First heating	Second heating	First heating	Second heating	First heating	Second heating
PCL raw	385.76 ± 0.91	−61.82 ± 1.05	−61.66 ± 1.51	59.38 ± 0.68[a]	58.37 ± 1.08	57.40 ± 2.22[a]	49.10 ± 2.06
PCL_1	385.47 ± 1.10	−58.26 ± 1.46	−62.69 ± 0.76	65.02 ± 1.19	57.11 ± 0.85	69.76 ± 2.91	50.05 ± 2.27
PCL/HA_1	347.26 ± 11.18[a]	−58.58 ± 1.12	−62.67 ± 0.37	63.92 ± 0.87	57.89 ± 0.54	70.07 ± 1.88	49.40 ± 1.36
PCL_1-CS/γPGA	378.76 ± 2.29[a]	−59.99 ± 1.71	−62.55 ± 0.43	64.74 ± 0.91	60.12 ± 2.50	68.14 ± 5.05	48.31 ± 2.62

Data expressed as average ± standard deviation ($n = 3$).
[a] Value significantly different compared to those of other scaffold types.

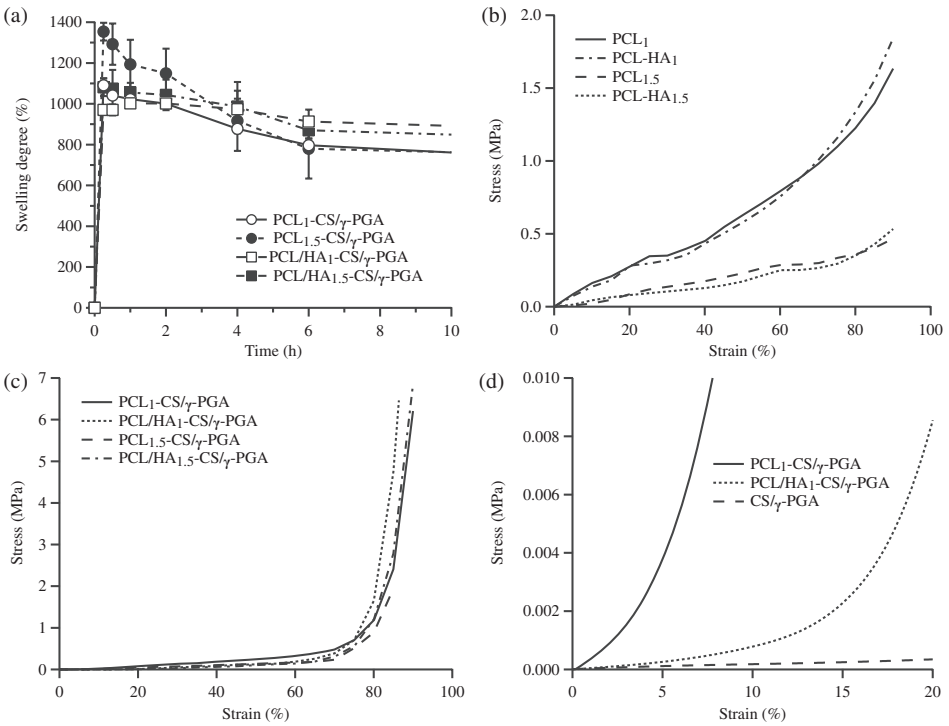

Figure 5. Swelling and mechanical behavior evaluation of the developed scaffolds: (a) swelling degree (SD) curves of the optimized biphasic constructs in DMEM at 37 °C. Representative compressive stress–strain curves of the developed scaffolds: (b) PCL based samples; (c) biphasic constructs; (d) biphasic constructs *versus* CS/γ-PGA hydrogel (strain rate 1 mm min^{-1} and maximum strain 90%; PBS 1× at 37 °C).

be assumed that the experimental procedure for biphasic scaffold preparation did not alter the macromolecular architecture of wet-spun PCL.

Determination of the swelling degree

The swelling properties of the optimized biphasic scaffolds were studied in DMEM at 37 °C (Fig. 5(a)). As expected by virtue of the hydrophobic nature of PCL, the SD of the PCL scaffolds investigated at different time intervals up to 10 h of soaking gave no appreciable values and thus PCL was not included in the graphic representation of the samples' swelling behavior. All the analyzed samples showed similar SD curves characterized by a maximum value after 30 min of immersion and reaching equilibrium within a few hours (Fig. 5(a)). Scaffolds produced by employing a d_{xy} of 1.5 mm were characterized by a significantly higher SD in the first few hours, probably due to the larger pore size as well as the lower PCL ratio in the biphasic construct. No significant differences were recorded between HA-loaded and unloaded biphasic scaffolds. The observed decrease of the SD within the first hour of soaking could be attributed to a partial loss of the polyanion component that is not involved in the formation of the PEC hydrogel. However, the good stability of the hydrogel phase penetrating the PCL fibrous structure is supported by the observed constant weight of the samples up to 10 h.

Equilibrium swelling of PEC hydrogels is determined by the balance between the elastic retractile response of the polymeric network and the net osmotic pressure within the network due to the mobile counterions around the fixed charge groups.[59] In the equilibrium swollen state, the biphasic constructs increased their weight up to 10-fold due to culture medium absorption by the hydrogel phase. The observed swelling values are comparable to those reported for porous CS/γ-PGA PEC hydrogels obtained by different techniques, such as freeze drying and CAWS,[33,34] suggesting that the presence of the PCL layered structure does not remarkably affect the ability of the construct to absorb an aqueous medium. This swelling ability could be exploited in tissue engineering strategies requiring scaffold absorption of large amounts of physiological fluids.

Table 3. Mechanical parameters of the investigated scaffolds and a CS/γ-PGA hydrogel

Scaffold	*E* (MPa)	Stress at 50% strain (MPa)	Stress at 90% strain (MPa)
PCL_1	1.3401 ± 0.1923	0.6858 ± 0.0524	2.0599 ± 0.4039
$PCL_{1.5}$	0.2158 ± 0.0350	0.2203 ± 0.0350	0.5208 ± 0.0643
PCL/HA_1	1.2375 ± 0.2282	0.4880 ± 0.2282	1.5886 ± 0.4041
$PCL/HA_{1.5}$	0.2932 ± 0.0250	0.1861 ± 0.0116	0.5368 ± 0.0125
PCL_1-CS/γ-PGA	0.1472 ± 0.0808	0.2305 ± 0.0155	4.3294 ± 2.5378
$PCL_{1.5}$-CS/γ-PGA	0.0907 ± 0.0614	0.1205 ± 0.0185	1.5299 ± 1.0886
PCL/HA_1-CS/γ-PGA	0.0348 ± 0.0114	0.1657 ± 0.0426	3.2829 ± 2.7545
$PCL/HA_{1.5}$-CS/γ-PGA	0.0249 ± 0.0046	0.0941 ± 0.0137	5.1500 ± 2.1911
CS/γ-PGA hydrogel	0.0014 ± 0.0005	0.0047 ± 0.0039	0.1930 ± 0.1231

Data expressed as average ± standard deviation ($n = 5$).

Mechanical properties

The compressive mechanical properties of the developed scaffolds were evaluated using an unconfined uniaxial testing machine. Representative stress–strain curves of PCL and PCL/HA scaffolds are reported in Fig. 5(b). Scaffolds produced employing $d_{xy} = 1$ mm had significantly higher compressive modulus and strength than scaffolds produced employing $d_{xy} = 1.5$ mm because of the higher fiber packing density (Table 3). Although previous studies have shown that HA inclusion into a polymeric matrix fiber scaffold can lead to enhanced mechanical properties,[29,36,60] an unequivocal effect of HA loading on the compressive parameters of the developed scaffolds was not observed. As examples, while in the case of $PCL_{1.5}$ scaffolds an increased modulus upon HA loading was observed, in the case of PCL_1 scaffolds significantly lower modulus and strength were measured for loaded scaffolds.

All the tested biphasic scaffolds showed a similar compressive behavior characterized by a slow increase of the stress up to around 60% strain, followed by a region with a fast increase of the slope of the curve (Fig. 5(c)). In comparison to PCL scaffolds, the biphasic constructs showed a lower compressive strength up to around 80% strain and a much higher strength in the subsequent region. In addition, the biphasic scaffolds displayed a stiffness 10- to 100-fold that of the CS/γ-PGA hydrogels (Fig. 5(d), Table 3).

Most of the studies aimed at the mechanical reinforcement of hydrogels with a fibrous polymeric network reported on the employment of electrospun non-wovens with a resulting increase of stiffness by 1- to 3-fold in comparison to the hydrogel phase.[61,62] Visser *et al.*[37] developed a mathematical model to study the mechanical behavior of a gelatin methacrylate with increased stiffness through the combination with a highly aligned ultrafine PCL fiber architecture obtained by melt-electrospinning writing. They demonstrated that under axial compression the hydrogel phase places the PCL fibers under tension with an overall result of increasing the stiffness up to 50-fold. Because of the incompressible nature of swollen polymers, each volume of the hydrogel phase confined into a scaffold cell expands in response to the applied stress causing fiber deformation. However, in the case of thicker fibers (>88 μm) mechanical reinforcement of the hydrogel was not achieved due to the stronger vertical column of fiber crossings causing water to flow out of the scaffold. Although the fiber size of the biphasic scaffolds reported in the present study is even larger (>200 μm), it is likely that the higher flexibility of microporous wet-spun fibers in comparison to dense fibers by melt processing[29] allowed a uniform deformation of PCL to be achieved with enhancement of the compressive strength of the biphasic construct.

Antimicrobial properties

The antibacterial activity of biphasic scaffolds against *S. epidermidis* ATCC 35984 and *E. coli* ATCC 25922 was evaluated by monitoring the bacterial growth in liquid cultures. As shown in Fig. 6, biphasic constructs were able to markedly inhibit the growth of both bacterial species. In particular, a 15-fold decrease in the OD_{600} value compared to the untreated control was observed for *S. epidermidis* after 8 h of incubation (Figs 6(a) while an approximately 4-fold reduction of optical density was assessed for *E. coli* after 6 h of incubation (Figs 6(b). Hence, the antibacterial effect of the biphasic scaffolds was compared with that of the PCL-based scaffolds and of the CS/γ-PGA hydrogel. For all time points tested, biphasic constructs caused a statistically significant reduction in the OD_{600} value compared to the PCL (and PCL/HA) scaffold, while no difference was observed compared to the CS/γ-PGA hydrogel.

The results suggested that the antimicrobial properties of the whole system are due to the presence of CS. The antimicrobial activity of CS against many Gram-positive and Gram-negative bacteria has been well documented in the literature.[63,64] Due to this bioactive property, CS has been previously investigated as scaffolding material in the clinical treatment of chronic periodontitis.[65] Although its exact mechanism of action is still unclear, it is likely that the polycationic structure of CS may interact electrostatically with the anionic components of the bacterial surface (e.g. lypopolysaccharide and peptidoglycan) and target the cell membrane, leading to cell damage or death.[55] A scaffold endowed with antimicrobial properties could generally be desired in order to respond to the elevated risk of infections from bacteria introduced during the surgical implantation.[66] In addition, the hours following an implantation procedure are crucial for the evolution of microbial infections, because the immune response is not active yet. A successful integration of the implanted scaffold with the host tissues is achieved only if a critical bacterial colonization of its surface is avoided. This becomes extremely challenging in the case of infection-related periodontal diseases caused by bacterial species able to form a biofilm resistant to antibiotics.[65] In this context, the use of CS in the hydrogel phase could be a very promising approach to inhibit the short-term bacterial colonization of the scaffold, thus favoring its integration into the periodontal defect site.

CONCLUSIONS

Combining a 3D PCL scaffold with a predefined porous architecture and good structural stability with a CS/γ-PGA PEC with

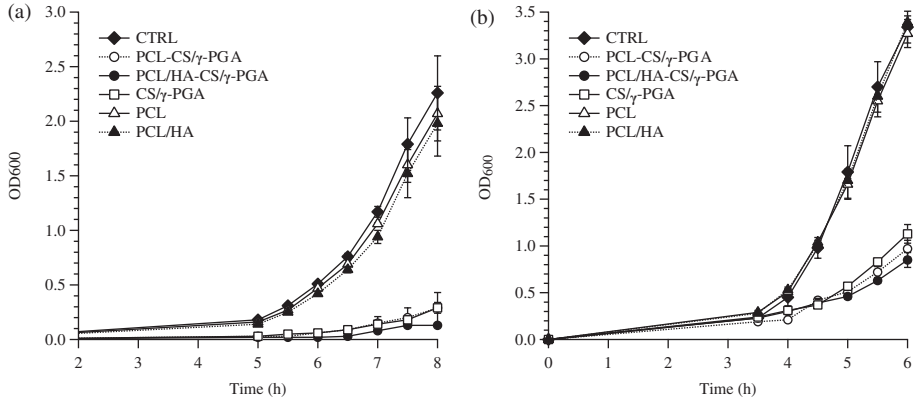

Figure 6. Antibacterial activity evaluation. Growth curves of *S. epidermidis* ATCC 35984 (a) and *E. coli* ATCC 25922 (b) in the presence of PCL-based scaffolds, biphasic constructs and CS/γ-PGA hydrogel. Controls (CTRL) represent untreated bacteria. Data are expressed as mean $\pm$ standard error of three independent experiments.

good swelling properties could represent a synergistic tool for the development of biphasic scaffolds suitable to be functionalized by platelet concentrate absorption. The developed experimental method is well suited for the production of PCL-CS/γ-PGA biphasic structures showing good integration at the macroscale and microscale. As demonstrated by the comparative mechanical characterization, the biphasic structures were characterized by enhanced mechanical properties in comparison with the hydrogel alone. This result was not previously observed in studies on AM PCL scaffolds with relatively large fiber size and can be attributed to the higher flexibility of wet-spun structures in comparison to melt-extruded structures as a consequence of the fiber sponge morphology. Furthermore, the presence of CS confers antibacterial properties to the biphasic scaffolds, representing a useful tool to minimize the risk of bacterial proliferation at the site of implants and prevent implant failure.

The present study opens new possibilities for the development of innovative strategies focused on periodontal bone regeneration through the employment of bioactive scaffolds functionalized with autologous platelet concentrates. Future studies will address the ability of the developed biphasic constructs to absorb platelet concentrates and to support cellular colonization *in vitro*. The possibility of obtaining anatomically shaped scaffolds by means of the developed preparation process is part of ongoing research.

ACKNOWLEDGEMENTS

This study was supported by a Tuscany region (Italy) funded project 'Nuovi Supporti Bioattivi a Matrice Polimerica per la Rigenerazone Ossea in Applicazioni Odontoiatriche (R.E.O.S.S.)' as part of the program POR CReO FESR 2007–2013 – Le ali alle tue idee. The authors are grateful to Dr Randa Ishak for her excellent support in recording SEM images.

REFERENCES

1 Pihlstrom BL, Michalowicz BS and Johnson NW, *Lancet* **366**:1809–1820 (2005).
2 Ford PJ, Gamonal J and Seymour GJ, *Periodontol 2000* **53**:111–123 (2010).
3 Chen F-M and Shi S, Periodontal tissue engineering, in *Principles of Tissue Engineering*, 4th edn, ed. by Vacanti R, Lanza R and Langer J. Academic Press, Boston, MA, pp. 1507–1540 (2014).
4 Abou Neel EA, Chrzanowski W, Salih VM, Kim H-W and Knowles JC, *J Dent* **42**:915–928 (2014).
5 Rios HF, Lin Z, Oh B, Park CH and Giannobile WV, *J Periodontol* **82**:1223–1237 (2011).
6 Ramseier CA, Rasperini G, Batia S and Giannobile WV, *Periodontol 2000* **59**:185–202 (2012).
7 Farag A, Vaquette C, Theodoropoulos C, Hamlet SM, Hutmacher DW and Ivanovski S, *J Dent Res* **93**:1313–1319 (2014).
8 Dan H, Vaquette C, Fisher AG, Hamlet SM, Xiao Y, Hutmacher DW *et al.*, *Biomaterials* **35**:113–122 (2014).
9 Ivanovski S, Vaquette C, Gronthos S, Hutmacher DW and Bartold PM, *J Dent Res* **93**:1212–1221 (2014).
10 Requicha JF, Viegas CA, Hede S, Leonor IB, Reis RL and Gomes ME, *J Tissue Eng Regener Med* DOI: 10.1002/term.1816. (2013).
11 Requicha JF, Viegas CA, Muñoz F, Azevedo JM, Leonor IB, Reis RL *et al.*, *Tissue Eng A* **20**:2483–2492 (2014).
12 Costa PF, Vaquette C, Zhang Q, Reis RL, Ivanovski S and Hutmacher DW, *J Clin Periodontol* **41**:283–294 (2014).
13 Park CH, Rios HF, Jin Q, Bland ME, Flanagan CL, Hollister SJ *et al.*, *Biomaterials* **31**:5945–5952 (2010).
14 Park CH, Rios HF, Jin Q, Sugai JV, Padial-Molina M, Taut AD *et al.*, *Biomaterials* **33**:137–145 (2012).
15 Vaquette C, Fan W, Xiao Y, Hamlet S, Hutmacher DW and Ivanovski S, *Biomaterials* **33**:5560–5573 (2012).
16 Rasperini G, Pilipchuk SP, Flanagan CL, Park CH, Pagni G, Hollister SJ *et al.*, *J Dent Res* **94**:153S–157S (2015).
17 Lee CH, Hajibandeh J, Suzuki T, Fan A, Shang P and Mao JJ, *Tissue Eng Part A* **20**:1342–1351 (2014).
18 Fawzy E-S, Paris S, Becker S, Neuschl M and De Buhr W, *J Clin Periodontol* **39**:861–870 (2012).
19 McGuire MK and Scheyer ET, *J Periodontol* **78**:4–17 (2007).
20 Pandit N, Malik R and Philips D, *J Indian Soc Periodontol* **15**:328–337 (2011).
21 Sell SA, Ericksen JJ and Bowlin GL, *Polym Int* **61**:1703–1709 (2012).
22 Hanna R, Trejo PM and Weltman RL, *J Periodontol* **75**:1668–1677 (2004).
23 Demir B, Şengün D and Berberoğlu A, *J Clin Periodontol* **34**:709–715 (2007).
24 Yamamiya K, Okuda K, Kawase T, Hata K-I, Wolff LF and Yoshie H, *J Periodontol* **79**:811–818 (2008).
25 Döri F, Huszár T, Nikolidakis D, Tihanyi D, Horváth A, Arweiler NB *et al.*, *J Periodontol* **79**:660–669 (2008).
26 Preeja C and Arun S, Saudi J *Dent Res* **5**:117–122 (2014).
27 Puppi D, Chiellini F, Dash M and Chiellini E, Biodegradable polymers for biomedical applications, in *Biodegradable Polymers: Processing, Degradation and Applications*, ed. by Felton GP. Nova Science, New York, pp. 545–560 (2011).
28 Woodruff MA and Hutmacher DW, *Prog Polym Sci* **35**:1217–1256 (2010).
29 Puppi D, Mota C, Gazzarri M, Dinucci D, Gloria A, Myrzabekova M *et al.*, *Biomed Microdevices* **14**:1115–1127 (2012).
30 Phipps MC, Clem WC, Grunda JM, Clines GA and Bellis SL, *Biomaterials* **33**:524–534 (2012).
31 Sun H, Mei L, Song C, Cui X and Wang P, *Biomaterials* **27**:1735–1740 (2006).
32 Zhu J and Marchant RE, *Expert Rev Med Devices* **8**:607–626 (2011).

33 Tsao CT, Chang CH, Lin YY, Wu MF, Wang J-L, Han JL *et al.*, *Carbohydr Res* **345**:1774–1780 (2010).
34 Puppi D, Migone C, Morelli A, Bartoli C, Gazzarri M, Pasini D *et al.*, *J Bioact Compat Polym* DOI: 10.1177/0883911516631355 (2016).
35 Billiet T, Vandenhaute M, Schelfhout J, Van Vlierberghe S and Dubruel P, *Biomaterials* **33**:6020–6041 (2012).
36 Mota C, Puppi D, Dinucci D, Gazzarri M and Chiellini F, *J Bioact Compat Polym* **28**:320–340 (2013).
37 Visser J, Melchels FPW, Jeon JE, van Bussel EM, Kimpton LS, Byrne HM *et al.*, Nat Commun ***6****: article 6933* (2015).
38 Shin SR, Bae H, Cha JM, Mun JY, Chen Y-C, Tekin H *et al.*, *ACS Nano* **6**:362–372 (2012).
39 Saez-Martinez V, Garcia-Gallastegui A, Vera C, Olalde B, Madarieta I, Obieta I *et al.*, *J Appl Polym Sci* **120**:124–132 (2011).
40 Maranchi JP, Trexler MM, Guo Q and Elisseeff JH, *Int Mater Rev* **59**:264–296 (2014).
41 Yodmuang S, McNamara SL, Nover AB, Mandal BB, Agarwal M, Kelly T-AN *et al.*, *Acta Biomater* **11**:27–36 (2015).
42 Moutos FT, Freed LE and Guilak F, *Nat Mater* **6**:162–167 (2007).
43 Liao IC, Moutos FT, Estes BT, Zhao X and Guilak F, *Adv Funct Mater* **23**:5833–5839 (2013).
44 Marijnissen WJCM, van Osch GJVM, Aigner J, van der Veen SW, Hollander AP, Verwoerd-Verhoef HL *et al.*, *Biomaterials* **23**:1511–1517 (2002).
45 Yu H-S, Won J-E, Jin G-Z and Kim H-W, *BioRes Open Access* **1**:124–136 (2012).
46 Pati F, Jang J, Ha D-H, Won Kim S, Rhie J-W, Shim J-H *et al.*, *Nat Commun* **5**:article 3935 (2014).
47 Schuurman W, Khristov V, Pot MW, Weeren PRv, Dhert WJA and Malda J, *Biofabrication* **3**:021001 (2011).
48 Lee H, Ahn S, Bonassar LJ and Kim G, *Macromol Rapid Commun* **34**:142–149 (2013).
49 Cha C, Soman P, Zhu W, Nikkhah M, Camci-Unal G, Chen S *et al.*, *Biomater Sci* **2**:703–709 (2014).
50 Agrawal A, Rahbar N and Calvert PD, *Acta Biomater* **9**:5313–5318 (2013).
51 Giannitelli SM, Mozetic P, Trombetta M and Rainer A, *Acta Biomater* **24**:1–11 (2015).
52 Puppi D, Zhang X, Yang L, Chiellini F, Sun X and Chiellini E, *J Biomed Mater Res B* **102**:1562–1579 (2014).
53 Hoffman AS, *Adv Drug Delivery Rev* **64**(Suppl):18–23 (2012).
54 Puppi D, Piras AM, Pirosa A, Sandreschi S and Chiellini F, *J Mater Sci Mater Med* **27**:44 (2016).
55 Jiang W, Shi J, Li W and Sun K, *J Biomater Sci Polym Ed* **24**:539–550 (2013).
56 de Britto D and Campana-Filho SP, *Thermochim Acta* **465**:73–82 (2007).
57 Singh J, Dutta PK, Dutta J, Hunt AJ, Macquarrie DJ and Clark JH, *Carbohydr Polym* **76**:188–195 (2009).
58 Horn MM, Martins VCA and de Guzzi Plepis AM, *Carbohydr Polym* **77**:239–243 (2009).
59 Kang H-S, Park S-H, Lee Y-G and Son T-I, *J Appl Polym Sci* **103**:386–394 (2007).
60 Gloria A, Russo T, De Santis R and Ambrosio L, *J Appl Biomater Biomech* **7**:141–152 (2009).
61 Coburn J, Gibson M, Bandalini PA, Laird C, Mao H-Q, Moroni L *et al.*, *Smart Struct Syst* **7**:213–222 (2011).
62 Tao X, Kyle WB, Mohammad ZA, Dennis D, Weixin Z, James JY *et al.*, *Biofabrication* **5**:015001 (2013).
63 Martínez-Camacho AP, Cortez-Rocha MO, Castillo-Ortega MM, Burgos-Hernández A, Ezquerra-Brauer JM and Plascencia-Jatomea M, *Polym Int* **60**:1663–1669 (2011).
64 Dash M, Chiellini F, Ottenbrite RM and Chiellini E, *Prog Polym Sci* **36**:981–1014 (2011).
65 Akıncıbay H, Şenel S and Yetkin Ay Z, *J Biomed Mater Res B* **80B**:290–296 (2007).
66 Mouriño V and Boccaccini AR, *J R Soc Interface* **7**:209–227 (2010).